Structures 56 (2023) 104926

Contents lists available at ScienceDirect

Structures

journal homepage: www.elsevier.com/locate/structures

Practical flexural design approach for one-way hybrid fiber-reinforced concrete slabs based on a parametric study on slenderness limits

Marc Sanabra-Loewe, David Garcia, Nikola Tošić *, Albert de la Fuente

Universitat Politècnica de Catalunya · BarcelonaTech (UPC), Jordi Girona 1–3, 08034 Barcelona, Spain

ARTICLE INFO

Keywords:
Deflection control
Minimum slenderness
Serviceability
Stiffness
Moment of inertia
Fibre reinforced concrete
One-way solid slabs

ABSTRACT

Fiber-reinforced concrete (FRC) is increasingly used for structural applications. Slabs are a particularly attractive use for FRC due to a potentially increased redistribution capacity, as well as the efficient cracking control that fibers provide. However, methods for reliably establishing slenderness limits of such elements are missing. Therefore, in this study, a previously developed closed-form solution for slenderness limits of hybrid FRC (HFRC) slabs (steel reinforcement bars and steel fibers) is presented and updated. Subsequently, a comprehensive parametric study on one-way solid slabs is performed, drawing clear conclusions on which parameters are the most influencing and offering a practical flexural design approach in the form of graphs and tables for determining minimum thicknesses of HFRC slabs that may be used as design aids for practitioners.

1. Introduction

Fiber reinforced concrete (FRC), i.e. concrete with uniformly distributed steel and/or macro-synthetic fibers, has been largely researched in the last three decades as a potential alternative or complement to concrete reinforced with steel bars. With a focus on characterizing the material, a large number of research papers has been published, with an important emphasis on ultimate limit state (ULS) studies on tensile strength, flexure strength and shear strength. Additionally, since the research on FRC experienced rapid growth, considerable attention was paid to crack control, whereas studies on deflection became relevant only in the las decade.

However, in the design of reinforced concrete buildings, including fibers or not as concrete reinforcement, ULS considerations have increasingly become secondary to serviceability limit state (SLS) requirements, in particular, deflections [1]. Namely, while, on average, increasingly higher strength concrete is used over the past decades, the increase in strength is not accompanied by a proportional increase in stiffness. Following architectural, use and operational requirements for larger spans and earlier removal of shoring during construction, concrete structures are increasingly sensitive to deflection, and SLS of deformation becoming a design governing state.

At the same time, deflection calculation methods can be time-consuming and imprecise [1]. However, deflection calculations are required at early stages of design, given that the size (depth) of reinforced concrete members under flexure is governed by deflection control requirements. That is why a rational design of flexural members, such as slabs, needs to start by knowing what is the minimum thickness or maximum slenderness ratios (span/height L/h or span/effective depth L/d) that guarantees a proper deflection control. Several methods and code provisions aimed at setting minimum thickness exist for long for reinforced concrete (RC) members, but these are missing for FRC or hybrid FRC (HFRC) members, i.e. members reinforced with a combination of fibers and steel bars. Some of such methods for RC members are also well suited to the iterative process of design required for optimization, and it has been demonstrated that their rationality enables those methods to be extended and adapted for FRC and HFRC.

From the mid-twentieth century, the most common deflection control methods used have been constant slenderness ratios L/n recommended in design codes. However, it has been shown that such simplified approaches can lead to either excessively heavy or excessively deformable elements, both being resource-inefficient use [2,3]. The importance of indirect deflection control methods was also proven for optimization of embodied carbon in buildings [4]. However, efficient deflection control methods are not straightforward to implement at early stages of design, given the iterative nature of reinforced concrete design where deflection calculation depends on the reinforcement ratio, and the reinforcement ratio depends on the depth of the member, which in turn depends on deflection control design.

Among the methods that have been developed to overcome this

* Corresponding author.
E-mail address: nikola.tosic@upc.edu (N. Tošić).

https://doi.org/10.1016/j.istruc.2023.104926
Received 13 May 2023; Received in revised form 17 July 2023; Accepted 18 July 2023

drawback, the one initially proposed by Rangan [5], and subsequently updated by Scanlon and Choi [6] and Scanlon and Lee [7] stands out as being one of the most versatile in allowing the direct choice of boundary conditions, span, load, concrete properties and allowable deflection criteria [3]. Despite the method was originally developed for and applied to reinforced concrete (RC) elements with solid rectangular cross-section, its rationality enables to adapt it to other cross-sectional geometries and to variants of the material. Recent years have seen a growing trend of innovative concretes being applied, with alternative/sustainable binders (alkali-activated concretes, limestone calcined clay cements, etc.), aggregates (recycled aggregate concrete) and reinforcement (micro and macro structural fibers, fiber reinforced polymer bar, textile reinforcement), with many of those already being included in new design codes such as the new Eurocode 2, FprEN 1992-1-1:2022 [8,9].

Among these, one of the most investigated and practically applied concretes has become fiber reinforced concrete (FRC). FRC has become a popular solution because of its numerous benefits such as improved fracture energy [10], crack control [11,12], behavior under fatigue loads [13–18] and redistribution capacity [19,20]. This has led to the application of FRC in various structural members such as precast tunnel segments [21–23], ground-supported slabs [24], retaining walls [25] and, more recently, flat slabs for structural floors [26–30]. It is precisely this last application that can offer the largest market perspective for FRC. But proper coverage of deflection control by design codes is still lacking [24].

In the first experimental constructions that have been erected including FRC slabs, fiber reinforcement has been designed aiming at totally or almost totally replacing steel reinforcing bars. This has led to designs with quite high amounts of fibers (≥100 kg/m^3 of steel macrofibres). Alternatively, this research team believes that potentially optimal solutions may be found by combining bars and fibers, i.e. by using HFRC rather than FRC. This belief is founded in the facts that bars are more efficient at resisting directional and localized forces (such as tension due to flexure), whereas fibers are more efficient at resisting volumetric forces (such as tension due to shrinkage or temperature). This statement was already experimentally proven in [24,29,31] for ULS. However, finding the right proportion of the two sorts of reinforcement is not obvious, and may probably only be found after more research and construction practice.

Thus, the aim of the current research is to offer practitioners a straightforward design approach for HFRC concrete floors by providing design aids to find the minimum depth for one-way HFRC slabs -based on SLS of deformability criteria- as a start point for their designs.

One of the first steps in this direction was the study by Tošić et al. [32] in which a closed-form solution was developed for the so-called „long“ method of Rangan-Scanlon, enabling direct calculation of the effective moment of inertia factor α (ratio of the effective moment of inertia I_e to the gross moment of inertia I_g). This parameter, α, ultimately enables the use of the „short” method of Rangan-Scanlon, that is a quite accurate and still fast method to predict the minimum slenderness of RC members under deflection, such as slabs. In their study [32], the authors also extended the method to FRC and hybrid FRC (HFRC) elements, providing only a preliminary comparison between RC and HFRC elements.

Below, a comprehensive parametric study of one-way solid HFRC slabs is performed, analyzing the effect of different parameters (boundary conditions, span, load, allowable deflection, effective depth, concrete compressive and tensile strength) on slenderness limits, determined by means of using the novel closed-form solution. The results of the parametric study are presented and analyzed. As a result, a set of graphs and tables are provided, that may serve as design tools for practitioners.

2. Closed form solution for HFRC slenderness limit calculation

2.1. Formulation for RC members

In this section, a brief summary of both the Rangan-Scanlon method as presented in [5,6] and the closed-form solution for α as developed in [32] are provided. The basis for the Rangan-Scanlon method is the incremental deflection, Δ_{inc}, calculation as defined in Equation (1):

$$\Delta_{inc} = \frac{\lambda_\Delta \kappa W_{sus} L^4}{384 E_c I_e} + \frac{\kappa W_{sl} L^4}{384 E_c I_e} \tag{1}$$

Where,

λ_Δ – long-term deflection multiplier for sustained loads, $= \xi/(1 + 50\bullet\rho')$, where ξ is a time dependent-factor provided graphically in ACI 318-19 [33] and ρ' is the compressive reinforcement ratio,

κ – deflection coefficient depending on boundary conditions (5, 1.4, 2, 48 for simply supported, both ends continuous, one end continuous, and fixed end cantilever conditions, respectively),

W_{sus} – all sustained loads (self-weight + superimposed dead loads + sustained fraction of live load),

L – span length,

E_c – modulus of elasticity of concrete,

I_e – effective moment of inertia,

W_{sl} – additional live load (sustained fraction of live load).

The key parameter in the expression is the effective moment of inertia I_e. If calculated according to ACI 318-19 [33], this is

$$I_e = \begin{cases} I_g & for\ M_a \le (2/3)M_{cr} \\ \dfrac{I_{cr}}{1 - \left(\dfrac{(2/3)M_{cr}}{M_a}\right)^2 \left(1 - \dfrac{I_{cr}}{I_g}\right)} & for\ M_a > (2/3)M_{cr} \end{cases} \tag{2}$$

Where,

I_g – moment of inertia of the gross concrete cross-section,

I_{cr} – moment of inertia of the fully cracked cross-section,

M_{cr} – cracking moment,

M_a – maximum moment on the cross-section due to service loads at the stage deflection is calculated.

For a rectangular cross-section, the cracking moment M_{cr} can be computed as

$$M_{cr} = W_g f_r = \frac{bh^2}{6} f_r \tag{3}$$

Where,

W_g – section modulus of the gross concrete cross-section,

f_r – modulus of rupture,

b – cross-section width,

h – cross-section height.

To obtain an expression in terms of a span-to-depth ratio based on Equation (1), the following is assumed:

1. Δ_{inc} is equated with the maximum allowable value of the incremental deflection $(\Delta_{inc})_{allow}$,
2. I_g is taken as $bh^3/12$, assuming a rectangular solid cross-section, and
3. I_e is taken as αI_g.

Then, the following holds:

$$(\Delta_{inc})_{allow} = \frac{12\lambda_\Delta \kappa W_{sus} L^4}{384 E_c \alpha b h^3} + \frac{12 W_{sl} L^4}{384 E_c \alpha b h^3} = \frac{\kappa}{32} \frac{(\lambda_\Delta W_{sus} + W_{sl}) L}{\alpha E_c b} \left(\frac{L}{h}\right)^3 \tag{4}$$

$$\frac{L}{h} = \left[\frac{32 \alpha E_c b}{\kappa(\lambda_\Delta W_{sus} + W_{sl})} \left(\frac{\Delta_{inc}}{L}\right)_{allow}\right]^{\frac{1}{3}} \tag{5}$$

The general or “long method of Rangan-Scanlon” consists of five steps [34]: 1] initial choice of h to account for self-weight (e.g., from current code-recommended L/h ratios), 2] calculation of required steel

area for strength requirements, 3] Calculation of I_e to determine α, 4] use of computed α in Equation (5), to find h and 5] check for convergence between obtained and assumed h and iterate until convergence.

Since the method is unsuitable for establishing element depths at early design stages—as it requires knowing the reinforcement ratio—the "short Rangan-Scanlon method" was proposed in posterior research, these consisting in adopting a preestablished value of α. A value of 0.4 was proposed by Scanlon and Choi [6] and 0.52 by Scanlon and Lee [7]. Still, adopting only a constant value of α can ben proven to be inaccurate or inadequate in certain cases [3].

Therefore, Tošić et al. [32] developed a novel closed-form solution to find α enabling a fast and easy use form of the "long method of Rangan-Scanlon", thus making feasible parametric studies that can facilitate finding a set of values of α to be finally used in the "short method of Rangan-Scanlon" (i.e. as recommended "constant" values).

First, Equation (2) is rewritten in dimensionless format with $\mu = M_{cr}/M_a$ and $\delta = I_{cr}/I_g$:

$$\frac{I_e}{I_g} = \alpha = \begin{cases} 1 for \mu \geq 1.5 \\ \dfrac{\delta}{1 - \left(\frac{2}{3}\mu\right)^2 (1-\delta)} for \mu < 1.5 \end{cases} \quad (6)$$

The cracking moment M_{cr} is rewritten as:

$$M_{cr} = \frac{bh^2}{6} f_r = \frac{bh^2}{6}\left(0.62\sqrt{f_c'}\right) = \frac{0.62}{6} bh^2 \sqrt{f_c'} (\text{Nmm}) \quad (7)$$

It should be noted that Equation (7) is valid only for SI units, for US customary units, 0.62 should be replaced by 7.5. Considering the required value of the tensile reinforcement ratio ρ_{req}, the applied moment $M_a = \eta M_n$ can be written as:

$$M_a = \eta M_n = \eta \left(\frac{d}{h}\right)^2 bh^2 \rho_{req} f_y \left(1 - \frac{\rho_{req} f_y}{1.7 f_c'}\right) (\text{Nmm}) \quad (8)$$

Where,

M_n – nominal flexural strength

η – ratio of maximum moment due to service loads to nominal flexural strength

d – distance from extreme compression fiber to centroid of longitudinal tension reinforcement,

f_c' – specified compressive strength of concrete,

f_y – specified yield strength of reinforcement,

ρ_{req} – tensile reinforcement ratio required to resist M_n (at midspan for simply supported and continuous members and at the support for cantilevers).

For the case of SI units, μ can be written as:

$$\mu = \frac{M_{cr}}{M_a} = \frac{0.62\sqrt{f_c'}}{6\eta \left(\frac{d}{h}\right)^2 \rho_{req} f_y \left(1 - \frac{\rho_{req} f_y}{1.7 f_c'}\right)} \quad (9)$$

Whereas, for US customary units 0.62 should be replaced by 7.5.

As for $\delta = I_{cr}/I_g$, it is calculated from $I_g = bh^3/12$.

For an RC cross-section under bending moments (without an axial force), the position of the neutral axis is independent of the applied M and can be expressed through the neutral axis coefficient $\xi = c/d$, where c is the depth of the compressed zone through Eq. (10).

$$I_{cr} = \frac{bh^3}{12}\left[12\left(\frac{d}{h}\right)^3 n\rho_{prov}(1-\xi)\left(1 - \frac{\xi}{3}\right)\right] (\text{mm}^4) \quad (10)$$

Where,

n – ratio of steel-to-concrete moduli of elasticity (E_s/E_c).

ρ_{prov} – provided tensile reinforcement.

Thus, δ can be determined by means of Eq. (11).

$$\delta = \frac{I_{cr}}{I_g} = 12\left(\frac{d}{h}\right)^3 n\rho_{prov}(1-\xi)\left(1 - \frac{\xi}{3}\right) \quad (11)$$

For RC sections under bending including only tensile reinforcement and under service load, ξ can be directly computed with Eq. (12).

$$\xi = -n\rho_{prov} + \sqrt{(n\rho_{prov})^2 + 2n\rho_{prov}} = n\rho_{prov}\left(-1 + \sqrt{1 + \frac{2}{n\rho_{prov}}}\right) \quad (12)$$

Therefore, using Equations (9), (11) and (12), α can be calculated as a function of the specified concrete strength (from which E_c is determined), steel grade (from which f_y and E_s are determined), and an assumed (or calculated) amount of provided reinforcement ratio ρ_{prov}.

For low-reinforced cross-sections, the required amount of tensile reinforcement (ρ_{req}) may be less than the minimum amount of reinforcement (ρ_{min}) that must be provided to avoid brittle failure under tensile stress:

$$\rho_{min} = \max\left(\frac{0.25\sqrt{f_c'}}{f_y}, \frac{1.38}{f_y}\right) \text{for SI units}$$

$$\rho_{min} = \max\left(\frac{3\sqrt{f_c'}}{f_y}, \frac{200}{f_y}\right) \text{for US customary units} \quad (13)$$

Therefore, the provided amount of tensile reinforcement, ρ_{prov}, is defined according to Eq. (14).

$$\rho_{prov} = \max(\rho_{req}, \rho_{min}) \quad (14)$$

2.2. Formulation for HFRC members

The principal idea behind the use of HFRC instead of RC is to use fibers as a distributed reinforcement guaranteeing a minimum post-cracking (residual) flexural strength over the entire element with longitudinal steel reinforcement added in those zones where the largest bending moments (hogging or sagging) are expected [11,26,35], while ensuring that $M_{n\text{-}HFRC} \approx M_{n\text{-}RC}$.

The ACI 544.4-18 Guide to Design with Fiber-Reinforced Concrete [36] allows the calculation of the flexural strength of HFRC members by directly assuming the superposition of the flexural strength of both the RC and the FRC section, i.e., $M_{n\text{-}HFRC} = M_{n\text{-}RC} + M_{n\text{-}FRC}$. Additionally, the ACI 544.4-18 guide suggests the use of the *fib* Model Code 2010 [37] constitutive models for FRC.

Therefore, the moment bearing capacity of rectangular FRC cross-section may be calculated using the rigid-plastic model of the *fib* Model Code 2010, this resulting in Eq. (15).

$$M_{n-FRC} = 0.5 bh^2 f_{Ftu} (\text{Nmm}) \quad (15)$$

Where,

f_{Ftu} – ultimate residual tensile strength of FRC, $= f_{R3}/3$, where,

f_{R3} – residual flexural tensile strength corresponding to a crack mouth opening displacement (CMOD) value of 2.5 mm in the EN 14651 [38] three-point bending characterization test.

Then, the moment bearing capacity of an HFRC rectangular cross-section can be computed by applying Eq. (16).

$$M_{n-HFRC} = \left(\frac{d}{h}\right)^2 bh^2 \rho_{req} f_y \left(1 - \frac{\rho_{req} f_y}{1.7 f_c'}\right) + 0.5 bh^2 f_{Ftu} =$$

$$= bh^2\left[\left(\frac{d}{h}\right)^2 \rho_{req} f_y \left(1 - \frac{\rho_{req} f_y}{1.7 f_c'}\right) + 0.5 f_{Ftu}\right] (\text{Nmm}) \quad (16)$$

Where,

ρ_{req} – tensile reinforcement geometrical ratio (A_s/A_c), in the shape of bars, required to resist the remainder of M_n after the contribution of fibers is considered, i.e. $M_{n\text{-}HFRC} - M_{n\text{-}FRC}$ (at midspan for simply supported and continuous members and at the support for cantilevers).

Subsequently, for SI units, μ changes to μ_{HFRC} through a constant addition of $0.5 f_{Ftu}$ to the nominal flexural strength:

$$\mu_{HFRC} = \frac{\frac{0.62}{6} bh^2 \sqrt{f_c'}}{\rho_{req,HFRC} bh^2 \left[\left(\frac{d}{h}\right)^2 \rho_{req,HFRC} f_y \left(1 - \frac{\rho_{req,HFRC} f_y}{1.7 f_c'}\right) + 0.5 f_{Ftu} \right]} =$$

$$= \frac{0.62\sqrt{f_c'}}{6\eta \left[\left(\frac{d}{h}\right)^2 \rho_{req,HFRC} f_y \left(1 - \frac{\rho_{req,HFRC} f_y}{1.7 f_c'}\right) + 0.5 f_{Ftu} \right]} \quad (17)$$

Whereas, for US customary units, 0.62 should be replaced by 7.5 Additionally, δ, changes as well because of the different value of I_{cr} for HFRC members. For this purpose, the expression proposed by Amin et al. [39] is considered:

$$I_{cr,HFRC} = \left[\frac{bc^3}{3} + nA_{s,prov,HFRC}(d-c)^2 \right] + nA_F \frac{(h-c)^2}{3} \left(\text{mm}^4\right) \quad (18)$$

Where,

$A_{s,prov,HFRC}$ – area of provided tensile reinforcement bars,

A_F – cumulative area of fibers in the cracked portion of the cross-section.

Starting from the formulation of A_F proposed by Amin et al. [39], Tošić et al. [32]—through a series of simplifications adopted for steel fiber reinforced concrete (SFRC), based on a database of experimental results—reached Eq. (19). The original expression from [39] was simplified by adopting average values of steel fiber aspect ratio, ultimate strength and modulus of elasticity (from a database of experimental results) as 65, 1.25 GPa and 200 GPa.

$$A_F = 3.46bh \frac{f_{R3}}{\sqrt{f_c'}} (1 - 0.9\xi_{HFRC}) 10^{-3} \quad (19)$$

So, Equation (18) can be rewritten as Eq. (20)

$$I_{cr,HFRC} = \frac{bh^3}{12} n \left[12 \left(\frac{d}{h}\right)^3 \rho_{prov,HFRC} (1 - \xi_{HFRC}) \left(1 - \frac{\xi_{HFRC}}{3}\right) + 0.014 \frac{f_{R3}}{\sqrt{f_c'}} (1 - 0.9\xi_{HFRC}) \right] \quad (20)$$

and the coefficient δ expressed through Eq. (21)

$$\delta_{HFRC} = n \left[12 \left(\frac{d}{h}\right)^3 \rho_{prov,HFRC} (1 - \xi_{HFRC}) \left(1 - \frac{\xi_{HFRC}}{3}\right) + 0.014 \frac{f_{R3}}{\sqrt{f_c'}} (1 - 0.9\xi_{HFRC}) \right] \quad (21)$$

Hence, once μ_{HFRC} is found using equation (17) and δ_{HFRC} is found using equation (21), the effective moment of inertia factor for HFRC members (α_{HFRC}) can be computed. However, Tošić et al. [32] concluded that Equation (6) cannot be directly applied to HFRC and Eq. (22) should be applied to compute α_{HFRC}.

$$\alpha_{HFRC} = \begin{cases} 1 for \mu_{HFRC} \geq 1.5 \\ \dfrac{\delta_{HFRC}}{1 - \left(\dfrac{2}{3}\mu_{HFRC}\right)^{m_{HFRC}} (1 - \delta_{HFRC})} for \mu_{HFRC} < 1.5 \end{cases} \quad (22)$$

Namely, the authors state that, as α provides the ratio of I_e/I_g averaged over the entire member length, it depends on: (1) the neutral axis position in individual cracked sections; (2) the extent of cracking and (3) on contribution of uncracked sections, i.e. tension stiffening. In general, the cracking pattern of HFRC members will be significantly different from that expected for RC members with the same ratio of longitudinal reinforcement [40]. Hence, in [32], the exponent m_{HFRC} was introduced and calibrated using numerical simulations as

$$m_{HFRC} = \begin{cases} 2\left(1 - \dfrac{f_{R1}}{f_r} \bullet (1 - 1.1\rho^*)\right); for \dfrac{f_{R1}}{f_r} \leq 1.0 \\ 2\rho^* \leq 1; for \dfrac{f_{R1}}{f_r} > 1.0 \end{cases} \quad (23)$$

Indicating by its two branches, the dependence of the exponent m_{HFRC} on whether the FRC post-cracking residual strength displays softening or hardening behavior. More details can be found in the study by Tošić et al. [32], however, it should be noted that the exponent was calibrated based on numerical studies and further experimental verification is needed.

Where,

f_{R1} – average value of residual flexural tensile strength corresponding to a crack mouth opening displacement (CMOD) value of 0.5 mm in the EN 14651 [38] three-point bending characterization test.

ρ^* – min(0.5%, $\rho_{prov,HFRC}$).

Finally, in HFRC members, even in pure bending, the position of the neutral axis is dependent of loading (and therefore of M), so that Equation (12) cannot be used, and an iterative process is necessary. To avoid this, Tošić et al. [32] conducted a parametric study comparing neutral axis positions of HFRC and RC members with the same reinforcement ratio and under the same bending moment and obtained a direct relationship between ξ_{RC} and ξ_{HFRC}:

$$\xi_{HFRC}/\xi_{RC} = \left\{ \begin{matrix} 1.14(\rho_{prov,HFRC})^{-0.62}, \rho_{prov,HFRC} \leq 1.0\% \\ -0.065\rho_{prov,HFRC} + 1.24, \rho_{prov,HFRC} > 1.0\% \end{matrix} \right\} \geq 1.0 \quad (24)$$

Thereby, a complete set of equations was provided for direct use for the "long method of Rangan-Scanlon" for HFRC members.

In terms of practical application, to avoid brittle failure, the minimum longitudinal steel reinforcement ratio for HFRC members, $\rho_{min,HFRC}$, was adopted according to the Annex L of the new Eurocode 2 [8] provisions. In this code, $\rho_{min,HFRC}$ for HFRC beams is the same as for RC beams. But for slabs, a reduction up to 50% is allowed following Eq. (25).

$$\rho_{min,HFRC} = \left\{ \begin{matrix} \rho_{min,RC} for beams \\ 0.5\rho_{min,RC} for slabs \end{matrix} \right. \quad (25)$$

Thus, for hybrid reinforced slabs, $\rho_{min,HFRC}$ is taken as:

$$\rho_{min,HFRC} = \max\left(\frac{0.125\sqrt{f_c'}}{f_y}, \frac{0.69}{f_y}\right) \text{for SI units}$$

$$\rho_{min,HFRC} = \max\left(\frac{1.5\sqrt{f_c'}}{f_y}, \frac{100}{f_y}\right) \text{for US customary units} \quad (26)$$

Therefore, the provided amount of tensile bars reinforcement, $\rho_{prov,HFRC}$, is defined as:

$$\rho_{prov,HFRC} = \max\left(\rho_{req,HFRC}, \rho_{min,HFRC}\right) \quad (27)$$

3. Parametric study on HFRC one-way solid slabs

In order to investigate the practical implications of the proposed method, a comprehensive parametric study was devised and performed to find values of the effective moment of inertia factor α and slenderness L/h for HFRC one-way solid slabs. The motivation was ultimately to develop practical design tools based on the parametric study results, that allow the set the minimum depth of one-way solid slabs at early stages of design.

For this purpose, the following parameters and values were considered in the parametric study:

- Rectangular cross-section, of breadth b and height h;

- Reinforcing steel with a specified yield strength f_y of 60 ksi (413.7 MPa);
- Three specified concrete strengths, f_c', of 3000, 4000 and 5000 psi (20.7, 27.6 and 34.5 MPa);
- Three average residual tensile strengths, f_{R1}, of 150, 450 and 750 psi (1.0, 3.1 and 5.2 MPa);
- Residual strength $f_{R3} = f_{R1}$ (based on [32,41])
- Relative effective depth, d/h, of 0.75, 0.85 and 0.95;
- Spans L of 15 and 35 ft (4.6 and 10.7 m);
- Superimposed surface loads Q of 80 and 160 psf (3.8 and 7.7 kN/m^2);
- Three boundary conditions – fixed–fixed (both ends continuous), fixed–pinned (one end continuous) and pinned–pinned (simply supported);
- Two incremental deflection limits for floors or roofs. One for floors or roofs supporting or attached to non-structural elements that are likely to be damaged by large deflections (deflection limit of $L/480$, a case called "damageable") and one for floors or roofs not likely to be damaged by large deflections (deflection limit of $L/240$, a case called "non-damageable").

In total, there were 7 parameters, leading to $3 \times 3 \times 3 \times 2 \times 2 \times 3 \times 2 = 648$ individual cases. For each case, α was calculated using the following procedure:

1. An initial height h_0 was assumed based on existing L/h ratios in ACI 318-19 [33];
2. From the superimposed surface load and self-weight (determined based on h_0) the nominal moment(s) in representative cross-section (s) is(are) determined and bar reinforcement ratio(s) $\rho_{req,HFRC}$ necessary for strength requirements is(are) calculated;
3. $\rho_{req,HFRC}$ is checked against $\rho_{min,HFRC}$ given by Equation (26);
4. ξ is calculated according to Equation (12) for RC and, then, ξ_{HFRC} to Equation (24);
5. μ_{HFRC}, δ_{HFRC} and m_{HFRC} are calculated based on Equations (17), (21) and (23) and considering $M_a = 0.67M_n$, i.e., $\eta = 0.67$;
6. α_{HFRC} is calculated according to Equation (22) for the representative cross-sections of the member (mid-span cross-section and both support cross-sections, depending on the boundary conditions). The overall factor α for the entire member is then calculated by averaging the factors for representative sections considering the bending moment law, i.e., the portions of length of hogging and sagging moments, which are 0 and 1 for simply supported elements, 0.25 and 0.75 for one end continuous boundary conditions and 0.42 and 0.58 for both ends continuous boundary conditions;
7. h is found using Equation (5) considering L, α, $(\Delta/L)_{allow}$, boundary conditions (expressed through the factor κ, which is 5.0, 2.0 and 1.4 for simply supported elements and elements with one or both ends continuous, respectively), E_c, long-term deflection multiplier ($\lambda_\Delta = 2$) for loads causing long-term deflections;
8. h is checked against h_0 and the process is repeated until convergence.

The process is summarized in the flowchart in Fig. 1.

The values of f_{R1} and f_{R3} adopted for the study (average values), as well as their relationship ($f_{R3} = f_{R1}$) are representative of steel fiber reinforced concrete at typical quantities of 0.25%–1.50% by volume of concrete. Nonetheless, these values and the relationship are based on the database from which they were obtained [32,41] and may differ in other concretes or other fiber types (such as macro-synthetic fibers), specifically they were obtained using a linear regression with a coefficient of determination R^2 of 0.9. Nonetheless, both parameters are left independent in the method so different values can be adopted if measured or considered appropriate. Additionally, as recognized by Tošić et al. [32], the long-term deflection multiplier λ_Δ might be different for HFRC relative to RC. In fact, adopting the same value as for RC is conservative since the presence of steel fibers can improve tension stiffening [42]. However, currently available experimental results are insufficient and

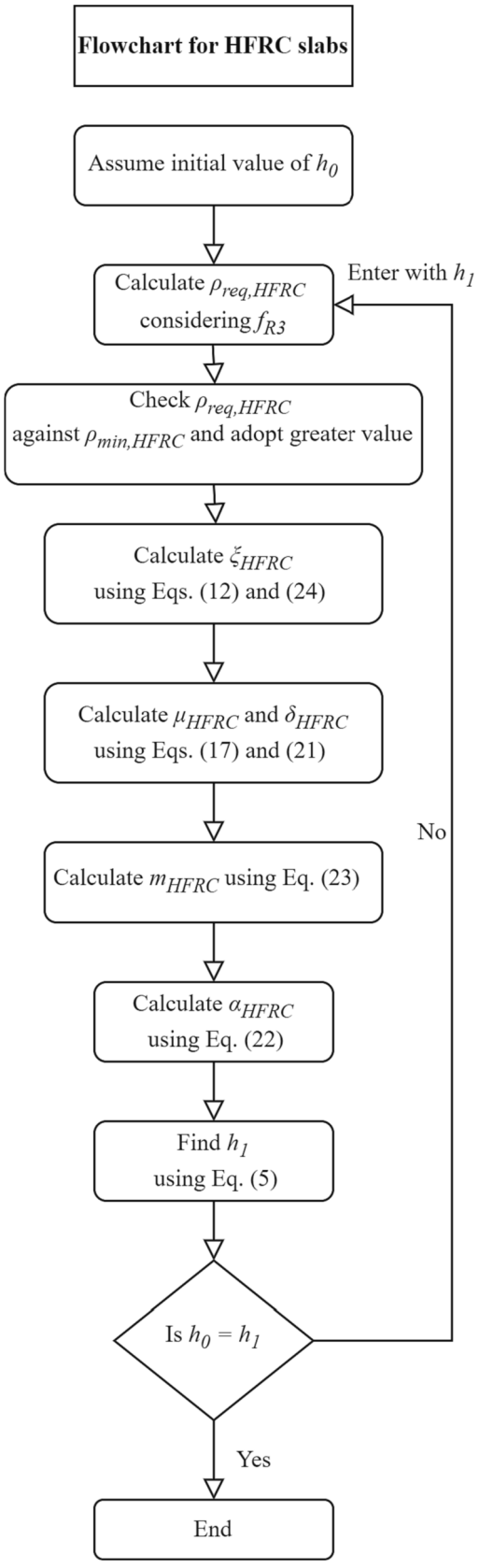

Fig. 1. Process flowchart for HFRC one-way slab design.

inconclusive in this regard.

For span and superimposed surface load, only two values were selected, covering the extremes of feasible ranges for usual one-way solid slabs in buildings. From Equation (5), it can be seen that the influence of these parameters on the value of $\alpha^{1/3}$ is linear and, therefore, any intermediate values could be omitted, as intermediate values may be linearly interpolated when searching for the slenderness (L/h) of a slab using equation (5), where L/h depends linearly of $\alpha^{1/3}$.

4. Results and discussion

After performing the parametric study calculations, the first next step was the analysis and the determination of the influence of individual parameters. In each case, six of the seven parameters were fixed and one was considered with its extreme values. For example, both ends continuous boundary condition, non-damageable non-structural elements, Q = 160 psf (7.7 kN/m^2), f_c' = 4000 psi (27.6 MPa), $f_{R1} = f_{R3}$ = 450 psi (3.2 MPa), $d/h = 0.85$. Then, spans L of 15 and 35 ft (4.6 and 10.7 m) are considered and the obtained L/h limits and α factors are compared for the two cases.

In this particular case, the L/h value for $L = 15$ ft (4.6 m) is obtained as 33.7 and for $L = 35$ ft (10.7 m) as 28.5. This is observed as a $|33.7/28.5 - 1| = 18.2\%$ difference, which is significant. However, if the value of α is considered for both cases, 0.323 and 0.301 are obtained, respectively. In this case, the difference should be analyzed in terms of $\alpha^{1/3}$, since this is how α influences L/h in Equation (5). Hence, the difference is $|(0.323/0.301)^{1/3} - 1| = 2.4\%$, much smaller than when considering L/h.

This process was then repeated for each of the individual parameters. Since seven parameters were considered in total, in order to obtain easy-to-use graphic charts, it was necessary to identify which parameters do not significantly affect the magnitudes of L/h or α. Once the less influential parameters were identified, the values of L/h or of α depending on those parameters are averaged as a single value of L/h or of α, respectively.

It was considered that when the difference between the two extreme values in a set of values of L/h or of $\alpha^{1/3}$ for a certain parameter is smaller than 10%, such a parameter is considered to be of negligible influence. By doing this, any error would have been limited to 5% with respect to each of the extreme values for which it was averaged. A 5% error on a slab with a depth of 250 mm (10 in) would be an error of 12.5 mm (0. 5 in). Such errors can be considered acceptable errors at an early stage of design.

After studying the sensitiveness of L/h and $\alpha^{1/3}$ to each of the parameters, it was consistently found that $\alpha^{1/3}$ was far less sensitive to variations to most of the parameters, and that it is a more robust variable. This finding is consistent with the results of prior research on RC members [32,34], where it was found that for slabs $\alpha^{1/3}$ is far less variable than L/h for flat elements (like slabs and wide beams), whereas L/h is less variable than $\alpha^{1/3}$ for deep elements (such as narrow beams).

Hence, the practical design charts developed below have been devised to find values of α rather than of L/h, since α could be expressed in terms of a smaller number of parameters (to which it is sensitive). Therefore, the slenderness (L/h) of a certain slab may be found by using Equation (5), i.e., using the "short method of Rangan-Scanlon," and using the corresponding value of α provided in the design tools.

After identifying the parameters to which $\alpha^{1/3}$ is more sensitive, it was found that the influence of the studied parameters varies significantly depending on whether slabs are attached to "damageable" or to "non-damageable" non-structural elements.

4.1. Slabs attached to "non-damageable" non-structural elements

For HFRC one-way solid slabs attached to "non-damageable" non-structural elements, the parameters significantly affecting $\alpha^{1/3}$ were found to be residual strength f_{R1}, load (Q), span (L) and boundary conditions. The large influence of boundary conditions and of span (L) were already expected, as these factors are among those that most influence the diagrams of forces and thus the level of cracking of the cross section, which influences the moment of inertia and thus α. The influence of load (Q) is often disregarded in design codes [8,33]. However, finding that it is influential on α was not a surprise in this case, as previous research reached the same conclusion [3,34]. The influence of residual strength f_{R1}, which was never put forward by a similar study, can well be explained by the fact that f_{R1} influences the depth of the position of the neutral axis of the cracked section. This, in its turn, influences the moment of inertia of the cracked section, and thus α.

The specified concrete compressive strength (f_c') was not significantly affecting $\alpha^{1/3}$. Despite the variation of the concrete compressive strength (f_c') considerably influences deflection through the modulus of elasticity (E_c), this influence is already considered in the method, because in Eq. (5) the modulus of Elasticity (E_c) is included as a parameter. So, as the variation of the modulus of elasticity (E_c) is not expected to influence α. Besides, the influence of the compressive strength (f_c') was found to be only of second order on α, through its influence on the modulus of rupture (f_r) and the residual strength f_{R1}.

At the same time, the relative effective depth, d/h, was found to be an "intermediately" significant parameter – depending on the combination of other parameters. It was found that d/h does not affect significantly $\alpha^{1/3}$ when the boundary condition is "both ends continuous". Whereas, for other boundary conditions ("one end continuous" and "simply supported"), in some cases d/h was only found to be influential when it becomes very small, i.e. $d/h = 0.75$. That is why the results for $d/h = 0.75$ have been separated from the results corresponding to $d/h = 0.85$ and 0.95 in those cases.

The results are shown in Table 1, where the α factor values are shown for each set of influential parameters, but averaged for the non-influential parameters. In other words, for a given set of f_{R1}, Q, L and boundary condition (and d/h, depending on the set of parameters), α was averaged for the compressive strengths and for d/h, where this parameter was found to be not predominant. This averaging was done

Table 1
Values of the α factor depending on several parameters for HFRC for one-way solid slabs attached to non-damageable non-structural elements.

α				Deflection control Att. to non-damageable elem. Q (psf)	
Boundary conditions	**L (ft)**	**f_{R1} (psi)**	**d/h**	**80**	**160**
Both ends continuous	15	150	All	0.284[a]	0.234[a]
		450	All	0.375[a]	0.330[a]
		750	All	0.429[a]	0.385[a]
	35	150	All	0.232[a]	0.209[a]
		450	All	0.333[a]	0.309[a]
		750	All	0.389[a]	0.364[a]
One end continuous	15	150	0.75	0.218	0.206
			0.85–0.95	0.198[a]	0.171[a]
		450	All	0.376[a]	0.284[a]
		750	All	0.376[a]	0.345[a]
	35	150	0.75	0.207	0.144
			0.85–0.95	0.164[a]	0.155[a]
		450	0.75	0.290	0.287
			0.85–0.95	0.277[a]	0.262[a]
		750	All	0.344[a]	0.329[a]
Simply supported	15	150	All	0.207[a]	0.182[a]
		450	All	0.324[a]	0.292[a]
		750	All	0.396[a]	0.363[a]
	35	150	0.75	0.191	0.190
			0.85–0.95	0.157[a]	0.148[a]
		450	0.75	0.282	0.271
			0.85–0.95	0.278[a]	0.262[a]
		750	All	0.351[a]	0.334[a]

[a] $\rho_{min,HFRC}$ (Equation (26)) is larger than $\rho^{+}_{req,HFRC}$.
NOTE: 1 ft = 0.305 m, 1000 psi = 6.895, 10 psf = 0.479 kN/m^2.

omitting the results for compressive strength, f'_c, equal to 4000 psi (27.6 MPa), and taking only the extreme values (3000 psi and 5000 psi, i.e. 20.7 and 34.5 MPa), as the small influence of compressive strength was found to be mostly linear and including the intermediate value did not make a difference. It can also be seen that, except for 10 cases (out of 46), the required positive reinforcement, $\rho^{+}_{req,HFRC}$ was smaller than $\rho_{min,HFRC}$, whereas $\rho^{-}_{req,HFRC}$ was always larger than $\rho_{min,HFRC}$ in slabs with either "one end continuous" or "both ends continuous".

The results in Table 1 are also graphically represented in Figs. 2–4 which allow a quick and easy determination of the value of α based on the influential parameters (load (Q), span (L), residual strength (f_{R1}), boundary conditions and sometimes d/h).

Finally, it should be noted that the whole set of values of α used to compute the average α values showed in Table 1 ranged from 0.140 to 0.437 with a global average of 0.290. It can be seen, therefore, that it is not possible to adopt a recommendation for a constant value of α, as the range of values is ± 50% of the average. Considering that L/h depends on $\alpha^{1/3}$, taking the average value of 0,290 would give an error of up to a 22% in L/h, which is well beyond the 5% that we have taken as acceptable.

4.2. Slabs attached to "damageable" non-structural elements

As for HFRC one-way solid slabs attached to "damageable" non-structural elements, the parameters significantly affecting $\alpha^{1/3}$ were found to be residual strength f_{R1}, load (Q), span (L) and boundary conditions. The specified concrete compressive strength (f_c') and the relative effective depth (d/h) did not significantly affect $\alpha^{1/3}$.

The results are shown in Table 2 where the α factor values are shown for each set of influential parameters, but averaged for the non-influential parameters. In this case, each value of α in Table 2 is an average of six values (averaging over the results for the two extreme values of f_c' and for the three values of d/h: 0.75, 0.85 and 0.95). For all 36 cases the required positive reinforcement, $\rho^{+}_{req,HFRC}$, was lower than the minimum amount of reinforcement, $\rho_{min,HFRC}$, defined by Equation (26).In 5 cases, also the required negative reinforcement, $\rho^{-}_{req,HFRC}$, was lower than the minimum, $\rho_{min,HFRC}$.

The results in Table 2 are also graphically represented in Figs. 5–7 which allow a quick and easy determination of the value of α based on the influential parameters (load (Q), span (L), residual strength (f_{R1}) and boundary conditions).

Finally, it should be noted that the whole set of values of α used to compute the average α values showed in Table 2 ranged from 0.207 to 0.601 with a global average of 0.401. As for slabs attached to non-damageable non-structural elements, it is not possible to adopt a recommendation for a constant value of α, as the range of values is ± 50% of the average. Considering that L/h depends on $\alpha^{1/3}$, taking the average value of 0,401 would give an error of up to a 20% in L/h, which is well beyond the 5% that we have taken as acceptable.

5. Conclusions

This study presented an in-depth analysis of the minimum slenderness calculation of SFRC hybrid one-way slabs, using the long method of Rangan-Scanlon. Some minor adjustments in the original formulas have been described. These adjustments where necessary to perform the parametric study, considering those cases where the minimum amount of reinforcement to prevent a brittle failure is larger than the reinforcement required without considering ductility requirements.

In order to identify and quantify the influence of residual flexural strength of the FRC (f_R) in HFRC one-way slabs, the study includes a representative range (from 150 to 750 psi, i.e. 1.0 to 5.2 MPa) for f_R. The results of the parametric study have been represented in plots and tables that can be used as design aids for practitioners. They are summarized next:

- For all the cases studied of one-way HFRC slabs, attached to either "damageable" or "non-damageable" non-structural elements, it was found that $\alpha^{1/3}$ is much less sensible than L/h to the variation of most of the studied variables. Therefore, all the results and the design tools provided allow the determination of α, that may subsequently be used to find L/h using the provided formulas of the long method of Rangan-Scanlon.

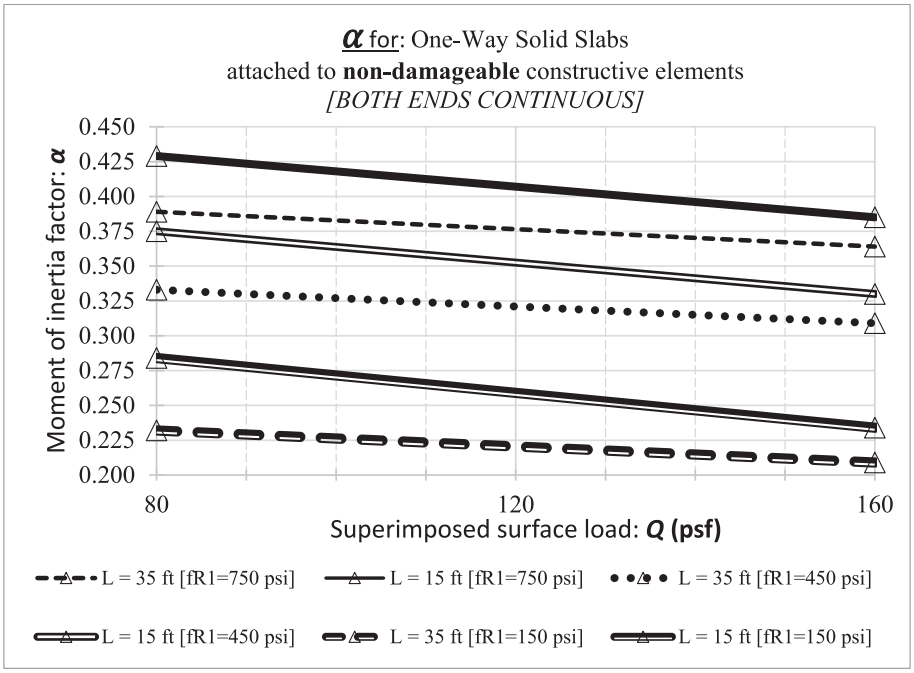

Fig. 2. HFRC one-way slabs with both ends continuous, attached to non-damageable non-structural elements– dependence of factor α on f_{R1}, span L and load Q (Δ– cases where minimum reinforcement, $\rho_{min,HFRC}$, is larger than the required positive reinforcement, $\rho^{+}_{req,HFRC}$). NOTE: 1 ft = 0.305 m, 1000 psi = 6.895, 10 psf = 0.479 kN/m^2.

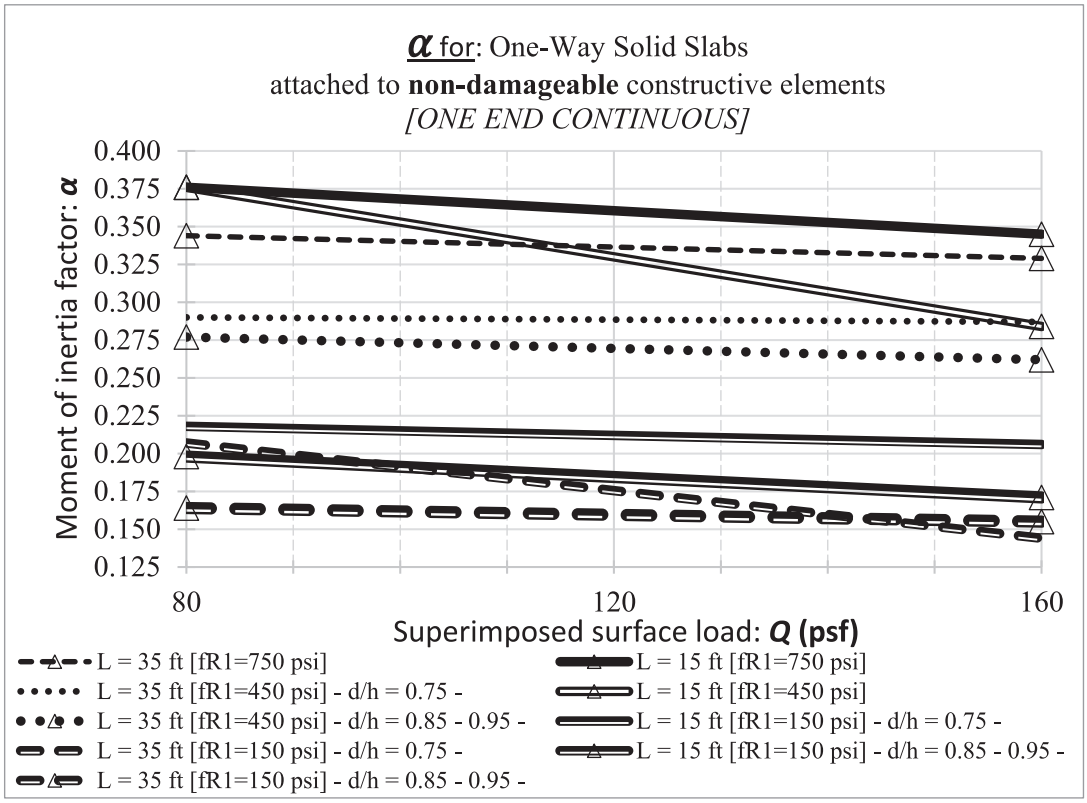

Fig. 3. HFRC one-way slabs with one end continuous, attached to non-damageable non-structural elements– dependence of factor α on f_{R1}, span L, load Q and d/h (Δ – cases where minimum reinforcement, $\rho_{\min,HFRC}$, is larger than the required positive reinforcement, $\rho^{+}_{req,HFRC}$). NOTE: 1 ft = 0.305 m, 1000 psi = 6.895, 10 psf = 0.479 kN/m^2.

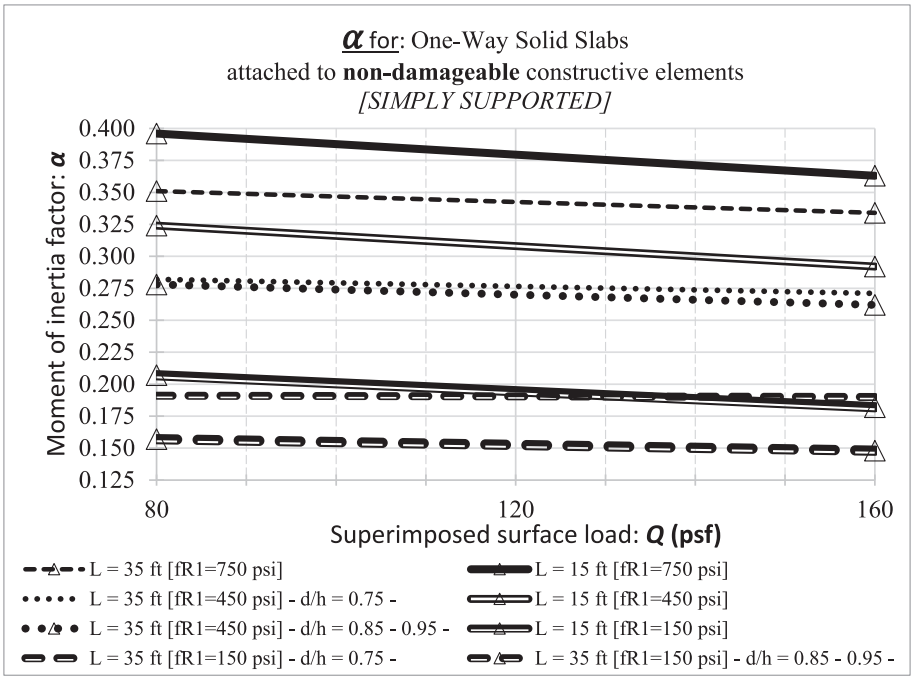

Fig. 4. HFRC simply supported one-way slabs, attached to non-damageable non-structural elements– dependence of factor α on f_{R1}, span L, load Q and d/h (Δ – cases where minimum reinforcement, $\rho_{\min,HFRC}$, is larger than the required positive reinforcement, $\rho^{+}_{req,HFRC}$). NOTE: 1 ft = 0.305 m, 1000 psi = 6.895, 10 psf = 0.479 kN/m^2.

Table 2
Values of the α factor depending on several parameters for HFRC one-way solid slabs attached to damageable non-structural elements.

α			Deflecion control Damageable	
			L (ft)	
Boundary conditions	***Q* (psf)**	**f_{R1} (psi)**	**15**	**35**
Both ends continuous	80	150	0.508[a]	0.388[a]
		450	0.557[a]	0.465[a]
		750	0.592[b]	0.513[b]
	160	150	0.398[a]	0.331[a]
		450	0.468[a]	0.416[a]
		750	0.514[b]	0.469[b]
One end continuous	80	150	0.332[a]	0.250[a]
		450	0.431[a]	0.363[a]
		750	0.492[b]	0.429[a]
	160	150	0.272[a]	0.225[a]
		450	0.376[a]	0.336[a]
		750	0.439[a]	0.401[a]
Simply supported	80	150	0.337[a]	0.240[a]
		450	0.453[a]	0.367[a]
		750	0.520[a]	0.441[a]
	160	150	0.282[a]	0.222[a]
		450	0.400[a]	0.344[a]
		750	0.468[a]	0.418[a]

[a] Minimum reinforcement, $\rho_{min,HFRC}$, after Equation (26), is larger than the required positive reinforcement, $\rho^{+}_{req,HFRC}$.
[b]Both positive and negative required reinforcements, $\rho^{-}_{req,HFRC}$ *and* $\rho^{-}_{req,HFRC}$, are lower than the minimum amount of reinforcement, $\rho_{min,HFRC}$.
NOTE: 1 ft = 0.305 m, 1000 psi = 6.895, 10 psf = 0.479 kN/m^2.

- In the case of HFRC one-way slabs attached to "damageable" non-structural elements:
  a. The parameters found to significantly affect $\alpha^{1/3}$ were load (Q), span (L), boundary conditions and residual flexural tensile strength (f_{R1}).
  b. For the range of considered parameters, α varied between 0.207 and 0.601 with an average of 0.401.
  c. For all the cases studied, the amount of positive reinforcement in bars needed to meet ductility requirements is larger than the amount of steel required for flexure strength. For a small number of cases this is also true for negative moments.
- In the case of HFRC one-way slabs attached to "non-damageable" non-structural elements:
  a. The parameters found to significantly affect $\alpha^{1/3}$ were load (Q), span (L), boundary conditions, residual flexural tensile strength (f_{R1}), and for certain combinations of the previous factors, relative effective depth (d/h) is also an influential factor.
  b. When the amount of fibers is high, i.e. $f_{R1} = 750$ psi (5.2 MPa), the relative effective depth (d/h) is not an influential factor. For lower amounts of fibers, the relative effective depth (d/h) is only influential for simply supported slabs and for slabs continuous at one end.
  c. For the range of considered parameters, α varied between 0.140 and 0.437 with an average of 0.290.
  d. With only very few exceptions, the amount of positive reinforcement in bars needed to meet ductility requirements is larger than the amount of steel required for flexure strength. Whereas, for negative moments, the amount of reinforcement required for flexure strength was found to be always larger than the minimum amount of steel required for ductility.

The results of this study, including the provided design tools, may be used in research focused on economic parameters, to find out whether hybrid reinforced HFRC one-way slabs may be economically competitive with conventional RC one-way slabs.

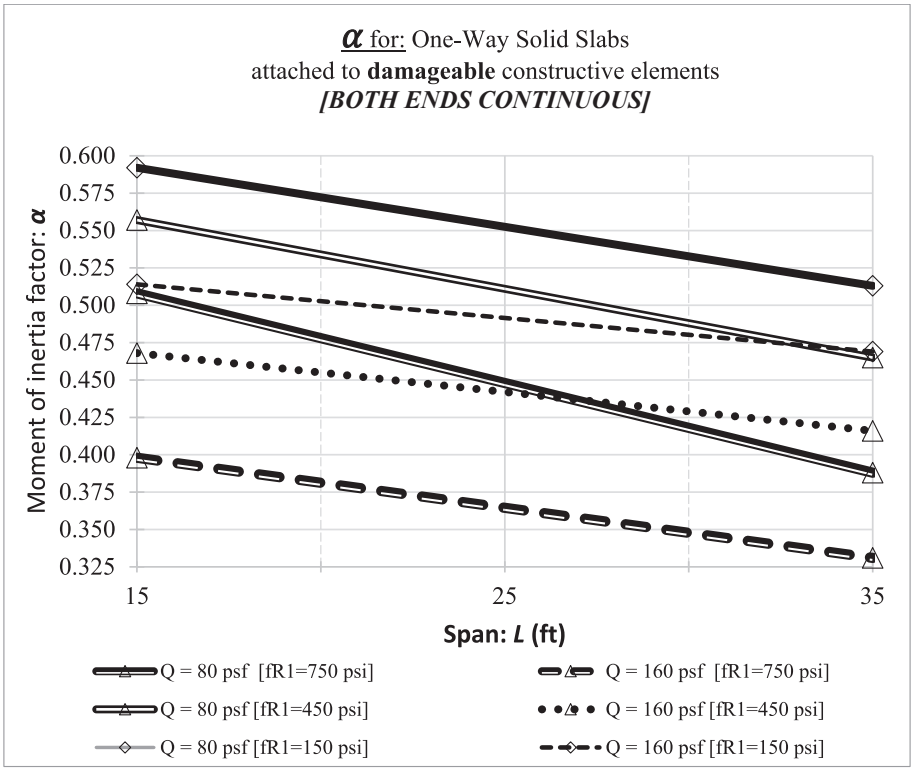

Fig. 5. HFRC one-way slabs with both ends continuous, attached to damageable non-structural elements – dependence of factor α on f_{R1}, span L and load Q (Δ – cases where minimum reinforcement, $\rho_{min,HFRC}$, is larger than required positive reinforcement, $\rho^{+}_{req,HFRC}$;◇– cases where minimum reinforcement, is larger than both the required positive moment, $\rho^{+}_{req,HFRC}$, and the required negative reinforcement, $\rho^{-}_{req,HFRC}$). NOTE: 1 ft = 0.305 m, 1000 psi = 6.895, 10 psf = 0.479 kN/m^2.

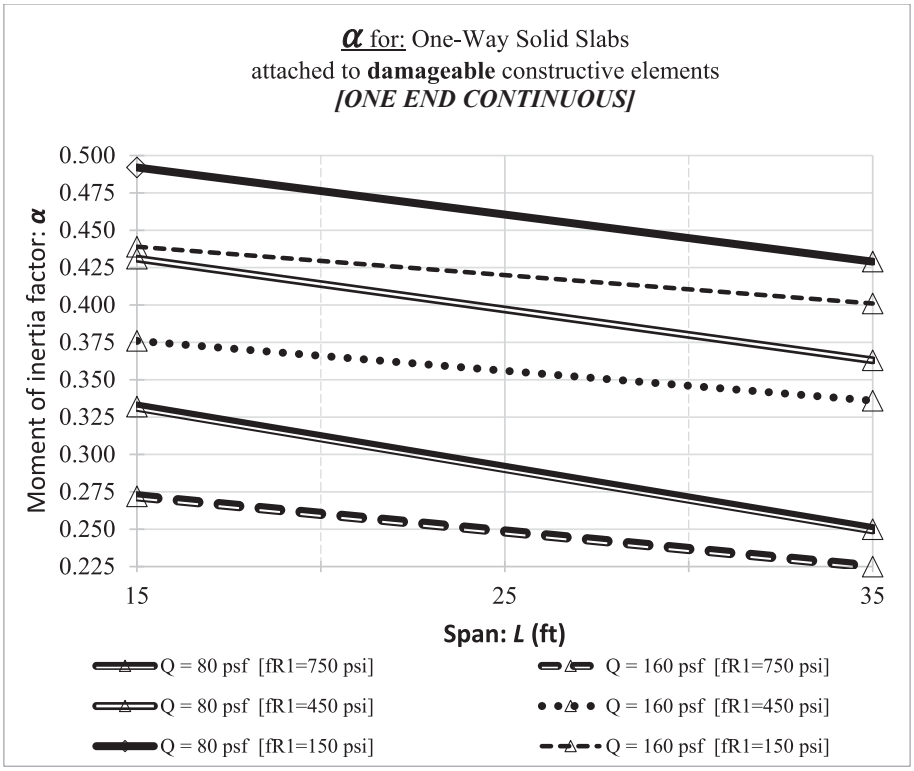

Fig. 6. HFRC one-way slabs with one end continuous, attached to damageable non-structural elements– dependence of factor α on f_{R1}, span L and load Q (Δ – cases where minimum reinforcement, $\rho_{\min,HFRC}$, is larger than the required positive reinforcement, $\rho^{+}_{req,HFRC}$; ◇– cases where minimum reinforcement, is larger than both the required positive moment, $\rho^{+}_{req,HFRC}$, and the required negative reinforcement, $\rho^{-}_{req,HFRC}$). NOTE: 1 ft = 0.305 m, 1000 psi = 6.895, 10 psf = 0.479 kN/m^2.

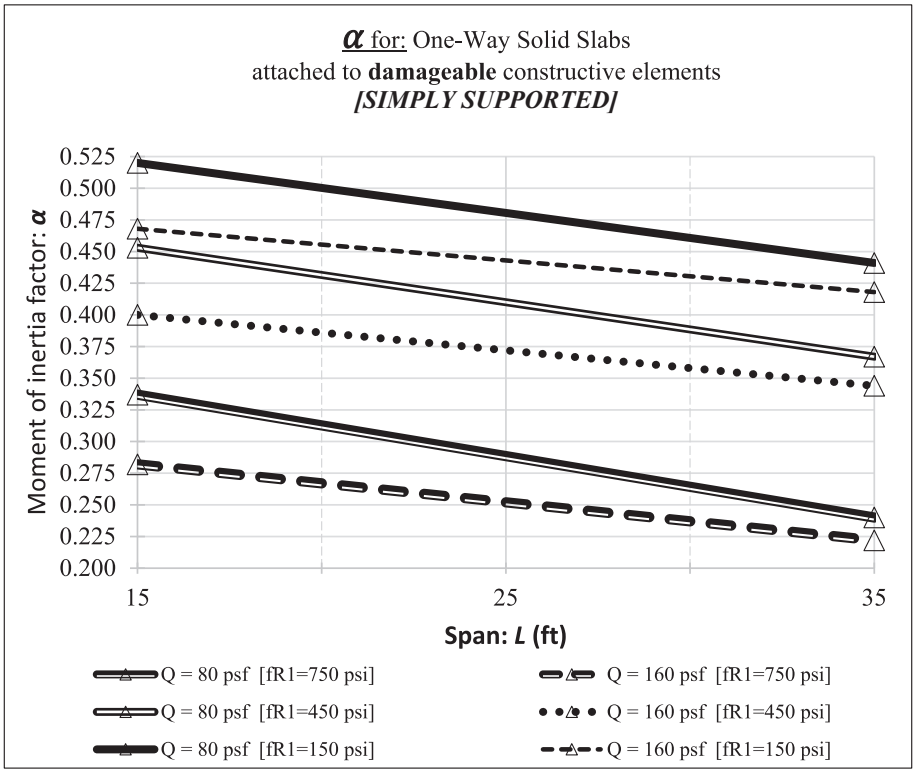

Fig. 7. HFRC simply supported one-way slabs, attached to damageable non-structural elements– dependence of factor α on f_{R1}, span L and load Q (Δ – cases where minimum reinforcement, $\rho_{\min,HFRC}$, is larger than required positive reinforcement, $\rho^{+}_{req,HFRC}$). NOTE: 1 ft = 0.305 m, 1000 psi = 6.895, 10 psf = 0.479 kN/m^2.

Funding

This research was funded by the Spanish Ministry of Science and Innovation under grant number PID2019-108978RB-C32 (CREEF). The APC was waived by the journal.

CRediT authorship contribution statement

Marc Sanabra-Loewe: Conceptualization, Methodology, Formal analysis, Writing – review & editing, Funding acquisition. **David Garcia:** Conceptualization, Formal analysis. **Nikola Tošić:** Methodology, Validation, Writing – original draft, Writing – review & editing. **Albert de la Fuente:** Resources, Visualization.

Declaration of Competing Interest

The authors declare that they have no known competing financial interests or personal relationships that could have appeared to influence the work reported in this paper.

References

[1] Beeby AW, Narayanan S. Designer's guide to Eurocode 2: Design of concrete structures. London: Thomas Telford; 2005.
[2] K.B. Bondy, Code deflection requirements - time for a change?, in: F. Barth, R. Frosch, H. Nassif, A. Scanlon (Eds.), Serv. Concr., American Concrete Institute, Farmington Hills, MI, 2005: pp. 133–145.
[3] Sanabra-Loewe M, Capellà-Llovera J, Ramírez-Anaya S, Pujadas-Gispert E. A path to more versatile code provisions for slab deflection control. Proc Inst Civ Eng - Struct Build 2023;176(4):272–86.
[4] Jayasinghe A, Orr J, Ibell T, Boshoff WP. Minimising embodied carbon in reinforced concrete flat slabs through parametric design. J Build Eng 2022;50:104136. https://doi.org/10.1016/j.jobe.2022.104136.
[5] Rangan BV. Control of beam deflections by allowable span-to-depth ratios. ACI J Proc 1982;79:372–7. https://doi.org/10.14359/10914.
[6] Scanlon A, Choi BS. Evaulation of ACI 318 minimum thickness requirements for one-way slabs. ACI Struct J 1999;96:616–22. https://doi.org/10.14359/699.
[7] Scanlon A, Lee YH. Unified span-to-depth ratio equation for nonprestressed concrete beams and slabs. ACI Struct J 2006;103:142–8. https://doi.org/10.14359/15095.
[8] FprEN 1992-1-1:2023, Eurocode 2: Design of concrete structures – Part 1-1: General rules, rules for buildings, bridges and civil engineering structures, CEN, Brussels, 2023.
[9] A. de la Fuente, A. Monserrat-López, N. Tošić, P. Serna, Design of Steel Fibre Reinforced Concrete Structures According to the Annex L of the Eurocode-2 2023, Hormigón y Acero. (2023). https://doi.org/10.33586/HYA.2023.3124.
[10] Zollo RF. Fiber-reinforced concrete: an overview after 30 years of development. Cem Concr Compos 1997;19:107–22. https://doi.org/10.1016/S0958-9465(96)00046-7.
[11] Pujadas P, Blanco A, De La Fuente A, Aguado A. Cracking behavior of FRC slabs with traditional reinforcement. Mater Struct Constr 2012;45:707–25. https://doi.org/10.1617/s11527-011-9791-0.
[12] Tiberti G, Minelli F, Plizzari G. Cracking behavior in reinforced concrete members with steel fibers: A comprehensive experimental study. Cem Concr Res 2015;68:24–34. https://doi.org/10.1016/J.CEMCONRES.2014.10.011.
[13] Carlesso DM, de la Fuente A, Cavalaro SHP. Fatigue of Cracked Steel Fibre Reinforced Concrete Subjected to Bending. RILEM Bookseries 2022;36:121–31. https://doi.org/10.1007/978-3-030-83719-8_11.
[14] Carlesso DM, Cavalaro S, de la Fuente A. Flexural fatigue of pre-cracked plastic fibre reinforced concrete: Experimental study and numerical modeling. Cem Concr Compos 2021;115:103850.
[15] Plizzari GA, Cangiano S, Alleruzzo S. THE FATIGUE BEHAVIOUR OF CRACKED CONCRETE. Fatigue Fract Eng Mater Struct 1997;20:1195–206. https://doi.org/10.1111/J.1460-2695.1997.TB00323.X.
[16] Zhang J, Stang H, Li VC. Experimental Study on Crack Bridging in FRC under Uniaxial Fatigue Tension. J Mater Civ Eng 2000;12:66–73. https://doi.org/10.1061/(ASCE)0899-1561(2000)12:1(66).
[17] J.-L. GRANJU, P. ROSSI, P. RIVILLON, G. CHANVILLARD, B. MESUREUR, A. TURATSINZE, Delayed behaviour of cracked SFRC beams, Fifth Int. RILEM Symp. Fibre-Reinforced Concr. (2000) 511–520.
[18] Stephen SJ, Gettu R. Fatigue fracture of fibre reinforced concrete in flexure. Mater Struct Constr 2020;53:1–11. https://doi.org/10.1617/S11527-020-01488-7/METRICS.
[19] A. Nogales, N. Tošić, | Albert De La Fuente, N. Tošić, A. de la Fuente, Rotation and moment redistribution capacity of fiber- reinforced concrete beams : Parametric analysis and code compliance, Struct. Concr. (2021) 1–20. https://doi.org/10.1002/suco.202100350.
[20] P. Schumacher, Rotation capacity of self-compacting steel fibre reinforced concrete, TU Delft, 2006.
[21] Conforti A, Trabucchi I, Tiberti G, Plizzari GA, Caratelli A, Meda A. Precast tunnel segments for metro tunnel lining: A hybrid reinforcement solution using macro-synthetic fibers. Eng Struct 2019;199:109628. https://doi.org/10.1016/J.ENGSTRUCT.2019.109628.
[22] la Fuente A, Pujadas P, Blanco A, Aguado A, De la Fuente A, Pujadas P, et al. Experiences in Barcelona with the use of fibres in segmental linings. Tunn Undergr Sp Technol 2012;27:60–71. https://doi.org/10.1016/j.tust.2011.07.001.
[23] Di Carlo F, Meda A, Rinaldi Z. Design procedure for precast fibre-reinforced concrete segments in tunnel lining construction. Struct Concr 2016;17:747–59. https://doi.org/10.1002/SUCO.201500194.
[24] Meda A, Plizzari GA, Riva P. Fracture behavior of SFRC slabs on grade. Mater Struct Constr 2004;37:405–11. https://doi.org/10.1617/14093.
[25] De La Fuente A, Aguado A, Molins C, Armengou J. Innovations on components and testing for precast panels to be used in reinforced earth retaining walls. Constr Build Mater 2011;25:2198–205. https://doi.org/10.1016/j.conbuildmat.2010.11.003.
[26] Aidarov S, Mena F, de la Fuente A. Structural response of a fibre reinforced concrete pile-supported flat slab: full-scale test. Eng Struct 2021;239:112292.
[27] Leporace-Guimil B, Mudadu A, Conforti A, Plizzari GA. Influence of fiber orientation and structural-integrity reinforcement on the flexural behavior of elevated slabs. Eng Struct 2022;252:113583. https://doi.org/10.1016/J.ENGSTRUCT.2021.113583.
[28] di Prisco M, Colombo M, Pourzarabi A. Biaxial bending of SFRC slabs: Is conventional reinforcement necessary? Mater Struct Constr 2019;52:1–15. https://doi.org/10.1617/s11527-018-1302-0.
[29] Facconi L, Plizzari G, Minelli F. Elevated slabs made of hybrid reinforced concrete: Proposal of a new design approach in flexure. Struct Concr 2019;20:52–67. https://doi.org/10.1002/SUCO.201700278.
[30] Nogales A, de la Fuente A. Numerical-aided flexural-based design of fibre reinforced concrete column-supported flat slabs. Eng Struct 2021;232:111745.
[31] Aidarov S, Tošić N, de la Fuente A. A limit state design approach for hybrid reinforced concrete column-supported flat slabs. Struct Concr 2022;23:3444–64. https://doi.org/10.1002/SUCO.202100785.
[32] Tošić N, Sanabra-Loewe M, Nogales A, de la Fuente A. Effective Moment of Inertia and Slenderness Limits of Reinforced Concrete and Fiber-Reinforced Concrete Slabs. ACI Struct J 2022;119:1–14.
[33] ACI 318-19, Building code requirements for structural concrete (ACI 318-19) and commentary, Farmington Hills, MI, 2019.
[34] M. Sanabra, A. Scanlon, Reinforced concrete predimensioning to enhance optimization, in: IABSE Symp. Eng. Progress, Nat. People, 2014: pp. 1626–1633. https://doi.org/10.2749/222137814814067978.
[35] Michels J, Waldmann D, Maas S, Zürbes A. Steel fibers as only reinforcement for flat slab construction - Experimental investigation and design. Constr Build Mater 2012;26:145–55. https://doi.org/10.1016/j.conbuildmat.2011.06.004.
[36] ACI Committee 544, Report on Fiber Reinforced Concrete, 2002.
[37] FIB, fib Model Code for Concrete Structures 2010, International Federation for Structural Concrete (fib), Lausanne, 2013. https://doi.org/10.1002/9783433604090.
[38] EN 14651, Test method for metallic fibred concrete — Measuring the flexural tensile strength (limit of proportionality (LOP), residual), Br. Stand. Inst. (2005). https://doi.org/9780580610523.
[39] Amin A, Foster SJ, Kaufmann W. Instantaneous deflection calculation for steel fibre reinforced concrete one way members. Eng Struct 2017;131:438–45. https://doi.org/10.1016/j.engstruct.2016.10.041.
[40] N. Tošić, M. Hunger, J.M. Vaquero, A. De La Fuente, Effect Of Sustained Load On The Flexural Bearing Capacity Of Polypropylene Fibre And Minimum Steel-Bar Reinforced Concrete Beams, in: Fib Congr. 2022 Concr. Innov. Sustain., fib, Oslo, 2022: pp. 1–12.
[41] Bairán JM, Tošić N, De La Fuente A. Reliability-based assessment of the partial factor for shear design of fibre reinforced concrete members without shear reinforcement. Mater Struct Constr 2021;54:185. https://doi.org/10.1617/s11527-021-01773-z.
[42] Amin A, Foster SJ, Watts M. Modelling the tension stiffening effect in SFR-RC. Mag Concr Res 2016;68:339–52. https://doi.org/10.1680/macr.15.00188.